Ageing of out-of-equilibrium nanoalloys by kinetic mean-field approach

Journal:	*Physical Chemistry Chemical Physics*
Manuscript ID:	CP-ART-01-2015-000600.R1
Article Type:	Paper
Date Submitted by the Author:	13-Mar-2015

Complete List of Authors:	Berthier, Fabienne; CNRS, Univ. Paris Sud, ICMMO/SP2M Tadjine, Athmane; Univ. Paris Sud, ICMMO/SP2M Legrand, Bernard; CEA, DEN, SRMP

Journal Name

RSCPublishing

ARTICLE

Ageing of out-of-equilibrium nanoalloys by kinetic mean-field approach

Cite this: DOI: 10.1039/xoxxooooox

F. Berthier[a,b], A. Tadjine[b], and B. Legrand[c]

Received ooth January 2012,
Accepted ooth January 2012

DOI: 10.1039/xoxxooooox

www.rsc.org/

This study describes the ageing of bimetallic nanoparticles using a kinetic mean-field method which provides the time evolution of the concentration for each site. We consider the cuboctahedron of 309 atoms in the Cu-Ag system, which is a prototype of systems with a strong tendency to phase separate. Starting from an initial homogenous configuration, we investigate the evolution towards the equilibrium configuration at different temperatures. Surprisingly, at low temperature, the kinetics exhibits a first transition towards an onion-like configuration followed by a second transition towards the equilibrium core-shell configuration. An analysis of the kinetics of the formation and then of the dissolution of the onion-like structure allows us to identify the main paths of the kinetic process.

1. Introduction

Nanoalloys present a wide range of technological applications in catalysis[1], optics[2] and magnetism[3]. Pure nanoparticles have unusual properties that vary with their size and their structure. By combining metallic species, the properties of nanoalloys may also vary with the chemical composition and a possible chemical ordering. The relationship between crystallographic and chemical structure and properties is the *leitmotif* that drives studies in this research field. Elaboration of nanoalloys with a well-controlled spatial distribution of the components is a great challenge. Different chemical configurations have been observed in nanoalloys, such as core-shell[4-8], onion-like[4,9], mixed[4,8] or Janus[4-7] configurations. For a same alloy, it is often possible to obtain different configurations depending on the elaboration process.[6,7] For instance, core-shell (with the A atoms in the core and the B atoms in the shell) or inverse core-shell (with the B atoms in the core and the A atoms in the shell) can be observed in the same A-B system by changing the order in the sequence of alternate deposition. The non-equilibrium configurations should evolve towards the thermodynamically stable configuration for sufficient long time. The ageing kinetics of nanoalloys is an open question of great interest as the spatial distribution of the components of the nanoparticles determines their properties and hence their technological applications. In particular, if an out-of-equilibrium configuration is elaborated due to specific properties, it is a key point to control its life time as a function of temperature. This requires a good knowledge of the thermodynamic driving forces that govern the kinetics and also of the diffusion process in the nanoalloys.

Numerical simulations are a powerful tool to study the kinetics at atomic scale and to provide a precious source of insight and fundamental knowledge, in particular in the absence of experimental characterisation of these kinetics. From the theoretical point of view, if the knowledge of the equilibrium chemical configuration of nanoalloys has given rise to a large number of studies,[10,11] this is not the case for the kinetics controlling the distribution of chemical elements in nanoparticles. Thus, we present in this paper one of the first studies of the kinetic path between an initial out-of-equilibrium configuration and the final equilibrium state.

For sake of simplicity, we investigate these kinetics in the framework of mean-field lattice gas model.[12] The limitations of mean-field approach of the kinetics are well-known,[13] but these models have the great advantage to allow one to explore large time scales and to be consistent with (mean-field) equilibrium thermodynamics. This ensures that the final state of the kinetics is really the equilibrium one, taking into account all the thermodynamic driving forces for superficial segregation and possible chemical ordering.[12] This type of approach has been largely used to study the kinetics of surface segregation in A_cB_{1-c} alloys or the kinetics of dissolution of a thin deposit of the A element on a B substrate.[14-17] Mean-field multilayer models have been developed by considering homogeneous concentrations per plane parallel to the surface, the possible in-plane inhomogeneity being not taken into account.[14-17] For nanoparticles, an equivalent approach would consist in describing the time evolution of the successive concentric

shells. However an additional difficulty comes from the fact that the number of sites differs for each shell, as the mean coordination number between two shells.[11,18,19] Moreover, previous studies[20,21] on equilibrium segregation in nanoalloys have shown that the concentrations can strongly differ between the different sites of the external shell (vertices, edges and facets). This implies to go beyond a homogeneous description of each shell and to adopt a more local description allowing one to obtain the time dependence of the concentration for *each site* of the nanoparticle. This is the so-called MFA-SK approach (Mean-Field Approximation, Site Kinetics).

The Cu-Ag system has been chosen due to the large number of experimental[22,23] and theoretical[14,15] studies describing the equilibrium and the kinetics of superficial segregation in semi-infinite alloys. Moreover, the equilibrium behaviour of Cu-Ag cuboctahedron has also been studied within the mean-field formalism.[18,21] A Cu core surrounded by an Ag shell is expected in a large range of temperature and concentration.[18-21] So, the aim of the present work is to illustrate the capabilities of the MFA-SK approach and to shed some light on how the equilibrium core-shell configuration is reached from an initial homogeneous configuration.

The organization of this paper is the following. In the second section, we describe the nanoparticle studied here, the energetic lattice-gas model and the MFA-SK approach allowing one to describe the time evolution of the concentration of each atomic site. We then present kinetics obtained from an initial homogeneous configuration at high and low temperatures (section 3). Conclusions are summarized in Sec. 4.

2. Mean-Field kinetic model

2.1. Cuboctahedron cluster

Among the various simple structures often considered in studying clusters of a few hundred of atoms, we chose the cuboctahedron based on the fcc structure, even if icosahedron, decahedron or truncated octahedron are generally more stable.[24,25] However, to control the ability of the kinetic MFA-SK method to reproduce the equilibrium state as the final one, it was a great advantage to use the same structure as in a previous work on the equilibrium segregation for the cuboctahedron with the magic size of 309 atoms.[26] This cluster, noted $Cubo_5$ hereafter, contains five concentric shells. Actually, for sake of simplicity, we grouped the central two shells, *i.e.*, the central atom and its 12 nearest neighbours, in a unique shell of 13 atoms (see fig. 1a). Thus, the number of sites for the different shells is equal to 162, 92, 42 and 13 when going from the surface (first shell) to the core shell (fourth shell).

Figure 1b shows the structure of the outermost shell. This shell is composed of 12 vertices (V), 24 edges 3 atoms each, 6 (001) facets 9 atoms each and 8 (111) facets 3 atoms each. Within a lattice-gas formalism, the number of broken bonds drives the superficial segregation. For the surface sites, this number of broken bonds is equal to 7 for the vertices, 5 for the edges, 4 for the (001) facets and 3 for the (111) facets.

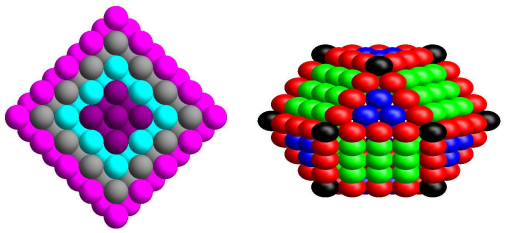

(a) **(b)**

Fig. 1 Cuboctahedron of order 5 (309 atoms): cross section (a) and view of the surface (b). In (a) the first shell (surface) is in magenta, the second shell in grey, the third shell in cyan and the core shell in purple. In (b), the vertices are in black, the edges in red, the (001) facets in green and the (111) facets in blue.

2.2. Lattice-gas model

First, we define the energetic quantities that characterize the system within the Ising model. For an alloy A_cB_{1-c}, the Hamiltonian of the system is written :[27]

$$H = \frac{1}{2}\sum_{i,j}\sum_{n,n\neq m} p_n^i p_m^j V_{nm}^{ij}\,, \qquad (1)$$

where V_{nm}^{ij} is the interaction between an atom of type i at a site n and an atom of type j at a site m ($i, j = A, B$). p_n^i is the occupation number that equals 1 if the site n is occupied by an atom of type i and 0 otherwise. For a binary alloy, $p_n^A = 1 - p_n^B$ and we set $p_n^A = p_n$, which leads to :

$$H = H_0 + \sum_n \sum_{m\neq n} p_n(\tau - V) + \sum_{n,m\neq n} p_n p_m V, \qquad (2)$$

n and m being sites in nearest-neighbour positions. H_0 is a constant $\left(H_0 = \sum_{n,n\neq m} V^{BB}/2\right)$, $\tau = (V^{AA} - V^{BB})/2$ is proportional to the difference between cohesive energies of pure metals and $V = (V^{AA} + V^{BB} - 2V^{AB})/2$ is the alloy pair interaction. V characterizes the tendency of the system to favor homoatomic ($V < 0$) or heteroatomic ($V > 0$) pairs.

The main features of the Cu-Ag system are well reproduced with the following values: $V = -30$ meV and $\tau = 46$ meV.[18,19] The negative value of V imposes a tendency to phase separate and the positive value of τ (Ag being less cohesive than Cu) leads to the Ag segregation on the less coordinated sites.[28,29]

2.3. Kinetic model

The kinetics is described by the mean field equations within the lattice-gas framework.[12] Usually a system is described as an ensemble of p classes of N_p crystallographically equivalent sites with homogeneous concentration c_p. For example, a semi-infinite system is described as a stacking of atomic planes parallel to the surface, each plane having the same number of atoms. By analogy, it should be tempting to consider the cluster as a stacking of concentric shells. However, the number of atoms differs from one shell to the other and all the sites within

a given shell are not equivalent, as previously mentioned for the outermost shell. Therefore we have chosen to consider the N sites of the nanoparticle individually; that means there are as many classes as atomic sites.

The time dependency of the concentration $c_p(t)$ of a site p is calculated as a detailed balance of incoming and outgoing fluxes between the site p and all the q-sites, which are in nearest-neighbour position of the site p :[30]

$$\frac{\partial c_p}{\partial\left(t/t_0\right)} = \sum_q \left[(1-c_p)c_q\gamma_{q\to p} - c_p(1-c_q)\gamma_{p\to q}\right], \qquad (4)$$

where $t_0 = a^2/D$, a being the lattice parameter and D the diffusion coefficient. D is written as $D = D_0\, exp(-Q/k_BT)$, where Q is the activation barrier for bulk diffusion and D_0 is the prefactor. $\gamma_{q\to p}$ is related to the transition probability for an exchange between an atom A in site p and an atom B in site q and is written as :[31,32]

$$\gamma_{q\to p} = exp\left(-\frac{\Delta H_p^{perm} - \Delta H_q^{perm}}{2k_BT}\right). \qquad (5)$$

ΔH_p^{perm} represents the permutation energy on site p, which is the energetic balance when changing an atom B in an atom A in this site. This energy is expressed in terms of the energetic parameters of the Ising model :[18,19]

$$\Delta H_p^{perm} = Z_p(\tau - V) + 2V \sum_q c_q, \qquad (6)$$

where Z_p is the coordination number for the site p, sites q being nearest-neighbours of the site p. Note that this definition of $\gamma_{q\to p}$ ensures the consistency between the steady state of this kinetic model and the equilibrium segregation profile obtained within the mean-field approximation.[14,15] To solve the system of N equations we use the NDSolve function of Mathematica with the help of the "EquationSimplification" method.[33]

The time evolution of the concentration of each site being known, it is possible to average the concentrations of all the (possibly inequivalent) sites of a given shell to obtain the concentration of this shell. Similarly, we can obtain the concentration of a class of crystallographically equivalent sites, as the vertices, the edges or the different facets of the outermost shell by averaging the concentration of all the sites belonging to this class. Note that this average may conceal inhomogeneous concentrations if crystallographically equivalent sites are no longer chemically equivalent. This has been already observed in this system in presence of chemical bistability for facets.[11,19-21] In this work we characterize the kinetics by means of the concentration per shell $\mathbb{C}_p$ and the concentration per type of surface site (vertices, edges, (001) and (111) facets) C_p, not without checking if the concentrations of all the sites of a same type are equal.

The numerical values of the prefactor and the activation energy for diffusion in the Cu-Ag system are $Q = 2.02$ eV/atom and $D_0 = 0.63$ cm^2/s.[22,23]

3. Results

Among all the kinetics we have studied, we have chosen to present the time evolution of a Ag_cCu_{1-c} nanoalloy, initially homogeneous, at high and low temperature. The nominal concentration we consider is $\boldsymbol{c = 0.35}$. The reason of this choice will appear in the presentation of the low temperature results.

High temperature

Firstly, we consider the high temperature regime (T = 1000 K), all the 309 sites of $Cubo_5$ having initially the same composition. As expected, the nanoparticle evolves toward its equilibrium state which corresponds to a surface shell enriched in Ag, the inner shells becoming almost pure in Cu (fig. 2a). More precisely, the radial concentration profile is monotonous, the second shell being slightly Ag-enriched with respect to the third and the core ones (fig. 2a). This monotonous profile is correlated to the negative sign of the alloy pair interaction (tendency to favour the homoatomic pairs).[11,28]

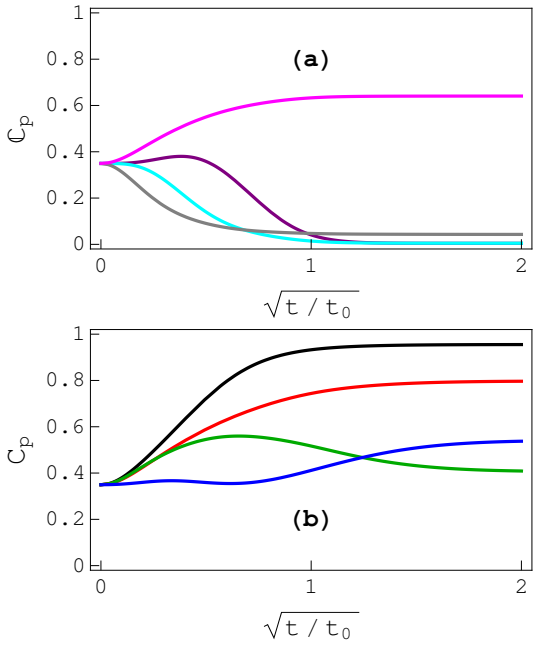

Fig. 2 Ageing kinetics at $T = 1000$ K for an initial homogeneous configuration of the $Cubo_5$ with $c = 0.35$. The Ag concentrations for the different shells (a) and for the different sites of the surface (b) are plotted as a function of the square root of the reduced time. In (a) the first shell (surface) is in magenta, the second shell in grey, the third shell in cyan and the core shell in purple. In (b), the vertices are in black, the edges in red, the (001) facets in green and the (111) facets in blue.

The kinetics begins with the increase of the surface concentration whereas the concentration of the second shell decreases. This is followed by the decrease of the concentration of the third shell and a slight increase of the concentration of the core shell. Then the core shell itself becomes almost pure Cu (fig. 2a). The time required to reach the equilibrium composition is almost the same for all the shells. However, we observe some exchanges between (001) and (111) facets, even after the times at which the surface concentration has reached its equilibrium value (fig. 2b). This delay to achieve the equilibrium between the different surface sites may disappear if

we take into account the acceleration of the diffusion at the surface. It is generally found that the activation energy is lower at the surface than in the core, this decrease being partially compensated by the decrease of the prefactor according to the Meyer-Neldel compensation law.[34,35] The equilibration between both types of facets is responsible of the non-monotonic time variation of the concentration of these facets. Note that the equilibrium Ag-segregation is higher for the (111) facets than the (001) one, while the number of broken bonds is smaller. This surprising result is related to the coupling with the edges, stronger for the (111) facets than fort the (001) one.[18]

Low temperature

Exploring the influence of temperature on the kinetics, one might expected that Ag atoms progressively migrate to the surface and cover the Cu aggregate in a similar way to the high temperature case. Fig. 3a shows that it is not the case : at T = 200 K, the change from the homogenous configuration to the equilibrium core-shell configuration passes through the formation of an onion-like structure!

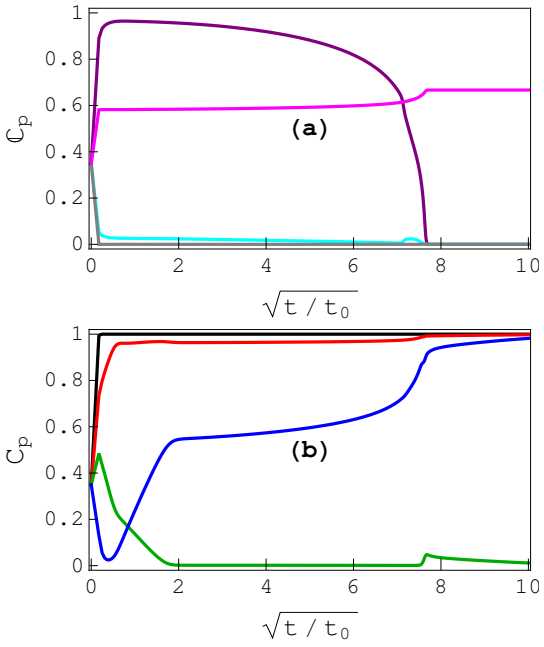

Fig. 3 Ageing kinetics at $T = 200$ K for an initial homogeneous configuration of the Cubo$_5$ with $c = 0.35$. The Ag concentrations for the different shells (a) and for the different sites of the surface (b) are plotted as a function of the square root of the reduced time. In (a) the first shell (surface) is in magenta, the second shell in grey, the third shell in cyan and the core shell in purple. In (b), the vertices are in black, the edges in red, the (001) facets in green and the (111) facets in blue.

Actually, the second and third shells become pure in Cu very rapidly, whereas the Ag atoms go mainly to the core which becomes almost pure in Ag. The surface is enriched also slightly in Ag, forming the onion-like structure: Ag – Cu – Cu – Ag (fig. 3a). This metastable configuration disappears at about $\sqrt{t/t_0} = 7.6$ (fig. 3a); the Ag atoms present in the core of the nanoparticle migrate to the surface. The second and third shells have a "transparent" behaviour: while they are traversed by copper and silver atoms, their concentrations remain almost constant. The Ag atoms diffuse from the core to fill the (111) facets of the surface, while the (001) facets remain almost pure in Cu (fig. 3b), due to the superficial local equilibrium.

As previously mentioned, the average concentrations for a class of sites can hide some heterogeneities between the sites belonging to a same class. This may be particularly the case when the average concentration of a class of sites is around 0.5 during the kinetics. For instance, for the (111) facets in the onion-like structure (cf. fig. 3b), this may correspond to some facets pure in Ag and some others pure in Cu. To clarify this point, we show the instantaneous concentration for each site of the surface in fig. 4, both before (fig. 4a) and after (fig. 4b) the dissolution of the onion-like structure. This figure confirms that all the (111) facets have the same concentration. This is also the case for the (001) facets. Moreover, all the sites of a given facet have the same composition, indicating that each facet is homogeneous.

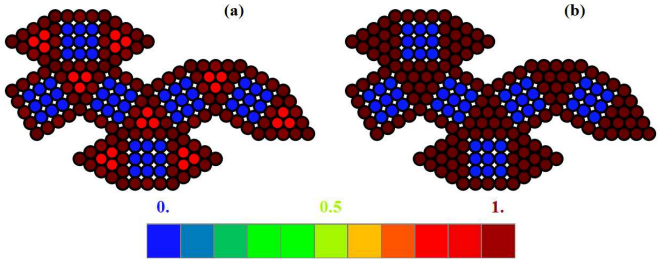

Fig. 4 Ageing kinetics at $T = 200$K for an initial homogeneous configuration of the Cubo$_5$ with $c = 0.35$. Instantaneous concentration for each site of the surface at $\sqrt{t/t_0} = 7$ (a) and $\sqrt{t/t_0} = 10$ (b). The color scale is indicated below the structure patterns of the Cubo$_5$.

In view of the metastability of the onion-like structure, is it possible to extend its life time by starting from a "perfect" onion structure for this composition? What we call the "perfect" onion structure is the structure obtained at very low temperature for this concentration, *i.e.* a mixed surface with pure Ag vertices and edges, equiatomic (111) facets and pure Cu (001) facets, second and third shells pure in Cu and pure Ag core shell. Fig. 5 shows that the life time is very similar to the one obtained by starting from the homogeneous configuration (see fig. 3): no gain in life time is obtained due to the perfect onion-like initial configuration; a slight decrease of this life time is even observed.

To identify the main diffusion paths during the dissolution of the onion-like structure, we have analysed the incoming and outgoing fluxes for each shell from Eq. (4) by determining the relative importance of the exchanges between the different sites of the shells p and $p + 1$. This analysis highlights the following short circuit diffusion path:

Core→Edges (shell 3)→Edges (shell 2)→F(111) (shell 1) (7)

Actually, Ag atoms leave the core to fill the (111) facets via the edge sites of the inner shells. To illustrate this point, we compare the kinetics of dissolution of the ideal onion-like configuration when exchanges only along the diffusion path (7) are allowed or when all exchanges are taken into account. The agreement between both kinetics is excellent and validates the proposed diffusion path. If we restrict the kinetics to other possible diffusion paths, the dissolution is much slower. For instance, for the path: Core → Edges (shell 3) → F(111) (shell 2) → F(111) (shell 1), the characteristic time is nearly twice longer.

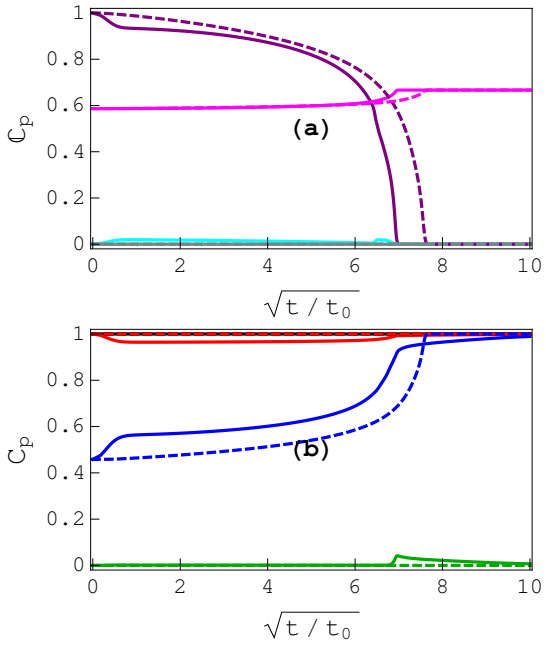

Fig. 5 Ageing kinetics at $T = 200$ K for an initial "perfect" onion configuration of the $Cubo_5$ with $c = 0.35$ when all exchanges between nearest neighbours are allowed (continuous lines) or by considering only the short circuit diffusion path (7) (dashed lines). The Ag concentrations of the different shells (a) and the different sites of the surface (b) are plotted as a function of the square root of the reduced time. In (a) the first shell (surface) is in magenta, the second shell in grey, the third shell in cyan and the core shell in purple. In (b), the vertices are in black, the edges in red, the (001) facets in green and the (111) facets in blue.

One can wonder what is the driving force for the dissolution of the onion-like structure? Is it due to a tendency to the surface to become more Ag-enriched or to the core to become Cu rich to avoid the Ag-Cu interface between the core and the third shell? Due to the "transparency" of the second and third shells, all the Ag atoms which leave the core arrive in the outermost shell and conversely all the Cu atoms which leave the surface arrive in the core. Thus, to know if this is the core or the surface which initiates the dissolution of the onion-like structure, we compare the fluxes between shells p and p+1 using Eq. (4).

Figure 6 shows that the flux between the core and the third shell displays a first peak at $\sqrt{t/t_0} \approx 7.1$, indicating that Ag atoms start to leave the core at this time. This occurs before the peak of the flux between the surface and the second shell (this peak being located at $\sqrt{t/t_0} = 7.6$, see fig. 6). This means that this is the instability of the Ag core, and not of the surface (and specially of the equiatomic (111) facets), that drives the dissolution of the onion-like structure.

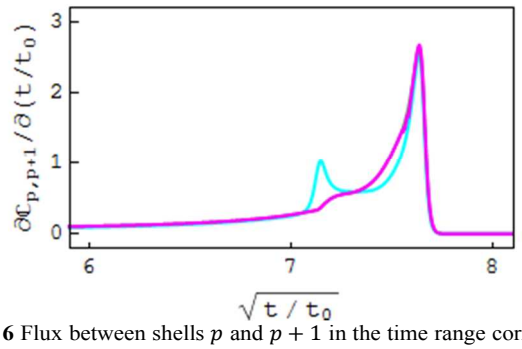

Fig. 6 Flux between shells p and $p + 1$ in the time range corresponding to the dissolution of the onion-like structure during the ageing kinetics at $T = 200$ K for an initial homogeneous configuration of the $Cubo_5$ with $c = 0.35$. In magenta: flux between the surface (p = 1) and the second shell which is indiscernible from the flux between the second and the third shell (not represented), in cyan flux between the third shell and the core.

It is interesting to compare the present behaviour to the one observed in A_cB_{1-c} thin films in equivalent conditions (*i.e.*, with a tendency to the element A to surface segregate, a strong tendency to phase separation and c < 0.5). Starting from a homogeneous state with a concentration located well inside the miscibility gap, *i.e.* in the spinodal regime, the kinetics of phase separation in the thin film present the following temporal sequence :[36]

i) an A surface enrichment with an A depletion in the underlayers and a labyrinth structure underneath (and the symmetric structure for the opposite surface of the thin film);
ii) the formation of a A – B – A sandwich (and the symmetric structure for the opposite surface of the thin film);
iii) the dissolution of the A precipitates in the center of the thin film to form the equilibrium phase separated configuration A (surface) – B (center) – A (surface).

Thus, the formation of the onion-like structure in the nanoparticle is completely equivalent to the second step of the phase separation kinetics observed in the thin films. The formation of a labyrinth structure in the first step of the kinetics is not observed for the $Cubo_5$, probably to its small size. Current work is in progress to see if a labyrinth structure appears at the beginning of the kinetics for nanoparticles of larger size.

A weakness of the present mean-field approach is to neglect the fluctuations of composition, contrary to Monte Carlo simulations for instance. To test the sensitivity of the kinetic pathway to fluctuations, we introduce an initial state with site concentrations equal to 1 or 0 (instead of c), using a random distribution, the nominal concentration remaining equal to c.

These fluctuations conserve the kinetic pathway leading to the metastable onion-like structure, but the pathway leading directly to the stable core-shell structure is also observed for some initial configurations. This points out the diversity of the possible kinetics in nanoalloys, even in a rigid lattice formalism. Taking into account the difference of size between atoms, as planned in future work, may increase this diversity as for infinite alloys.[37]

The present work has shown that, for a given concentration, there exists a critical temperature below which the onion-like structure may be is observed. Conversely, for a given temperature, is it possible to define a concentration range leading to the observation of the onion structure? To this aim, we perform systematic simulations at $T = 200$ K. The onion-like structure is observed for c belonging to the concentration range $0.1 - 0.7$. It is then possible to draw a metastable phase diagram (c, T) defining the domain of apparition of the onion-like structure starting from a homogenous initial state. This is, however, beyond the scope of the present paper, especially if one notes that the equilibrium phase diagrams of nanoalloys are still poorly understood.

Between the equilibrium phase diagram and the metastable phase diagram, the time dependency is added. In the present case, a time scale accessible to experiments, *i.e.*, from some minutes to some days, is obtained at intermediate temperatures (500-600 K). The onion-like structure is observed in this range of temperature for cluster of larger size, such as $Cubo_7$ (923 atoms). Note that the time scale may depend on the kinetic parameters which control the surface diffusion, even if the driving forces governing the metastability of the onion-like structure act mainly in the core and not at the surface.

4. Conclusions

This study of the ageing kinetics of initially homogeneous nanoalloys illustrates the ability of the mean-field kinetic equations applied to each atomic site to predict a rich variety of behaviours. Thus, for a system with a strong tendency to phase separate in the bulk and which presents a superficial segregation of one element, such as the Ag-Cu system, very different kinetics are observed at high and low temperature Whereas a progressive evolution towards the equilibrium core-shell configuration is observed at high temperature, the formation of a metastable "onion-like" structure is predicted at low temperature. The formation and then the dissolution of this metastable structure are shown to be similar to the behaviour observed in thin films and come from the competition between surface and bulk (or core) thermodynamic driving forces.

The kinetic mean-field approach used in this work allows one to analyse the fluxes between the different sites during the kinetics. This analysis emphasizes the role of the edges of the inner shells in the kinetic pathways leading to the dissolution of the onion-like structure.

The present work can be considered as a first step for the understanding of the kinetics in bimetallic nanoparticles. In cluster physics, a size-dependence is observed for a large number of properties. Therefore, works are in progress to determine how both the temperature below which the onion-like structure occurs and the life-time of this structure depend on the size of the nanoparticle. Ageing kinetics of other metastable nanostructures such as reverse core-shell configuration or Janus configurations are also among the perspectives of the present work.

Acknowledgements

It is a great pleasure to thank C. Mottet, G. Tréglia, J. Creuze, C. Andreazza and P. Andreazza for very fruitful discussions.

Notes and references

[a] CNRS, UMR 8182, F91405 Orsay Cedex, France.
[b] SP2M/ICMMO, Univ. Paris Sud, UMR 8182, F91405 Orsay Cedex, France.
[c] CEA, DEN, Service de Recherches de Métallurgie Physique, F91191 Gif-sur-Yvette Cedex, France.

1 J. Jellinek and E.B. Krissinel, *Theory of Atomic and Molecular Clusters*, Springer, Berlin, 1999.
2 U. Kreibig and M. Vollmer, *Optical Properties of Metal Clusters*, Springer, Berlin, 1995.
3 M. C. Froment, J. Morillo, M. J. Casanove and P. Lecante, *Europhys. Lett*., 2006, **73**, 885.
4 R. Ferrando, J. Jellinek and R. L. Johnston, *Chem. Rev*., 2008, **108**, 845.
5 T. Momin and A. Bhowmick, *J. Alloys. Compounds*, 2013, **559**, 24.
6 C. Langlois, D. Alloyeau, Y. Le Bouar, A. Loiseau, T. Oikawa, C. Mottet and C. Ricolleau, *Faraday Discuss*., 2008, **138**, 375.
7 C. Langlois, Z. L. Li, J. Yuan, D. Alloyeau, J. Nelayah, D. Bochicchio, R. Ferrando and C. Ricolleau, *Nanoscale*, 2012, **4**, 3381.
8 C. M. Gonzalez, Y. Liu and J. C. Scaiano, *J. Phys. Chem. C*, 2009, **113**, 11861.
9 D. Ferrer, A. Torres-Castro, X. Gao, S. Sepulveda-Guzman, U. Ortiz-Mendez and M. José-Yacaman, *Nano Lett.*, 2007, **7**, 1701.
10 F. Ducastelle, *Nanoalloys: synthesis, structure and properties,* chap. 5, Springer-Verlag, London, 2012.
11 J. Creuze, F. Berthier and B. Legrand, *Nanoalloys: synthesis, structure and properties,* chap. 6 , Springer-Verlag, London, 2012.
12 G. Martin, *Phys. Rev. B*, 1990, **41**, 2279.
13 R. E. Stoller, S. I. Golubov, C. Domain and C. S. Becquart, *J. Nucl. Mat.*, 2008, **382**, 77.
14 A. Saúl, B. Legrand and G. Tréglia, *Phys. Rev. B*, 1994, **50**, 1912.
15 A. Saúl, B. Legrand and G. Tréglia, *Surf. Sci.*, 1994, **307-309**, 804.
16 S. Delage, B. Legrand, F. Soisson and A. Saúl, *Phys. Rev. B*, 1998, **58**, 15810.
17 J.M. Roussel, A. Saúl, G. Tréglia and B. Legrand, *Phys. Rev. B*, 1999, **60**, 13890.
18 F. Lequien, J. Creuze, F. Berthier and B. Legrand, *J. Chem. Phys*., 2006, **125**, 094707.
19 F. Lequien, Thesis, Univ. Paris Sud, Orsay, 2008.

20 F. Lequien, J. Creuze, F. Berthier and B. Legrand, *Faraday Discuss*., 2008, **138**, 105.
21 F. Lequien, J. Creuze, F. Berthier, I. Braems and B. Legrand, *Phys. Rev. B*, 2008, **78**, 075414.
22 J. Eugène, G. Tréglia, B. Legrand, B. Aufray and F. Cabané, *Surf. Sci.*, 1991, **251-252**, 664.
23 J. Eugène, B. Aufray and F. Cabané, *Surf. Sci*., 1992, **251-252**, 372.
24 F. Baletto, R. Ferrando, A. Fortunelli, F. Montalenti and C. Mottet, *J. Chem. Phys.*, 2002, **116**, 3856.
25 C. Mottet, J. Goniakowski, F. Baletto, R. Ferrando and G. Tréglia, *Phase Transitions*, 2004, **77**, 101.
26 M. Lamloum, Internship report, Univ. Paris Sud, Orsay, 2010.
27 F. Ducastelle, *Order and Phase Stability in Alloys,* North-Holland, Amsterdam, 1991.
28 F. Berthier, B. Legrand and G. Tréglia, *Acta Mater.*, 1999, **47**, 2705.
29 V. Moreno, J. Creuze, F. Berthier, C. Mottet, G. Tréglia and B. Legrand, *Surf. Sci.*, 2006, **600**, 5011.
30 J. Philibert, *Diffusion et Transport de Matière dans les Solides*, Les Editions de Physique, Les Ulis, 1985.
31 A. Senhaji, G. Tréglia, B. Legrand, N. T. Barett, C. Guillot and B. Villette, *Surf. Sci*., 1992, **274**, 297.
32 A. Senhaji, Thesis, Univ. Paris Sud, Orsay, 1993.
33 Wolfram Research, Inc., Mathematica, Version 9.0, Champaign, IL (2012).
34 G. Boisven, L. J. Lewis and A. Yelon, *Phys. Rev. Lett*., 1995, **75**, 469.
35 G. Boisven and L. J. Lewis, *Phys. Rev. B*, 1996, **54**, 2880.
36 S. Delage, Thesis, Univ. Paris VI, Paris, 1998.
37 G. Abadias, A. Marty and B. Gilles, *Acta Mater.*, 1998, **46**, 6403.